

# FINITE ELEMENT MODEL OF BREAST COMPRESSION DURING MAMMOGRAPHY

J.H.Chung<sup>1</sup>, V.Rajagopal<sup>1</sup>, P.M.F.Nielsen<sup>1</sup>, M.P.Nash<sup>1</sup>  
<sup>1</sup>Bioengineering Institute, University of Auckland, New Zealand

**Abstract** – Diagnosis of the breast cancer involves the reconstruction of images taken during mammography, typically involving *cranio-caudal* (CC, or head-to-toe) and *medio-lateral oblique* (MLO, or shoulder-to-opposite hip) compression. Current algorithms to associate the two images are not appropriate for image registration due to the large non-homogenous deformation of the breast during a mammographic procedure. A finite element model of the breast which can simulate the breast mechanics under compression will help to establish the relations between the two images, making more effective tracking of tumours possible. We performed compression experiments on a cylindrical silicon gel phantom and compared experimental deformations with predictions from our computational framework, which incorporates contact mechanics with finite deformation non-linear elasticity. Using the known material properties of the gel, compression predictions matched closely with experimental results. We then performed compression experiments on a gel phantom moulded into a realistic anatomical breast shape to mimic mammography, and compared deformations with predictions using a patient specific finite element model. The combination of tissue mechanics with compression modelling has the potential to provide a virtual tool to track breast tumours, and to assist with surgical guidance for clinical procedures such as biopsy and radiotherapy.

## I. BACKGROUND

Breast cancer is the most commonly diagnosed cancer among women in Western societies, and it is becoming more frequently diagnosed in Eastern societies. Early detection increases the chances of survival. Currently one of the most commonly used procedures to diagnose breast cancer is mammography, which involves compression of the breast. Typically two separate images are taken, *cranio-caudal* (CC), and *medio-lateral oblique* (MLO). The detection of tumours can be achieved by reconstructing the image by combining these views. Non-rigid body transformation algorithms are commonly used in registering the images. However,

due to the large deformation of the breast when compressed, the images are subject to alignment errors as they do not take account of the physical laws of continuum mechanics. Rueckert et al. [1] used non-rigid body image alignment algorithms to register three-dimensional magnetic resonance images of the breast based on image characteristics. Tanner et al. [2] showed that by adding a simple volume preserving constraint, the alignment error was reduced. A finite element model of breast mechanics will potentially further improve the alignment accuracy by permitting only physically plausible transformations.

## II. MODELLING FRAMEWORK

### 2.1 Kinematics of Finite Deformations

During the mammographic procedure, breast tissues undergo deformations of up to 20%, hence it is necessary to model the mechanics with a finite deformation approach. We first define the deformation gradient tensor  $\mathbf{F}$  [3]:

$$\mathbf{F} = \frac{\partial \mathbf{x}}{\partial \mathbf{X}} \quad (1)$$

where  $\partial \mathbf{X}$  is a line segment in original or reference configuration, and  $\partial \mathbf{x}$  is the same material line segment after the deformation (i.e. the current configuration). From this deformation gradient, an important measure of deformation can be evaluated, the right Cauchy-Green strain tensor, defined to be:

$$\mathbf{C} = \mathbf{F}^T \mathbf{F} \quad (2)$$

In 3D space,  $\mathbf{C}$  is a 3 by 3, 2<sup>nd</sup> order tensor, and has three principle invariants:

$$\begin{aligned} I_1 &= \text{tr}(\mathbf{C}) \\ I_2 &= \frac{1}{2} \left[ (\text{tr}(\mathbf{C}))^2 - \text{tr}(\mathbf{C}^2) \right] \\ I_3 &= \det(\mathbf{C}) \end{aligned} \quad (3)$$

For an incompressible material,  $I_3$  (a measure of relative volume change) will be unity. From the right Cauchy-Green strain tensor, the Green Lagrangian strain tensor  $\mathbf{E}$  is calculated using

$$\mathbf{E} = \frac{1}{2}(\mathbf{C} - \mathbf{I}) \quad (4)$$

where  $\mathbf{I}$  is the identity matrix. This Green Lagrangian strain tensor is particularly important, as we assume that the silicon gel is a hyperelastic material for which the strain energy function  $W$  is a function of  $\mathbf{E}$ . The derivative of  $W$  with respect to  $\mathbf{E}$  yields the 2<sup>nd</sup> Piola-Kirchhoff stress tensor  $\mathbf{S}$ .

### 2.2 Soft Tissue Mechanics

From the principle of linear momentum, the equations of motion are derived [4]:

$$\text{div} \boldsymbol{\sigma} + \mathbf{b} = \rho \frac{d\mathbf{v}}{dt} \quad (5)$$

where  $\boldsymbol{\sigma}$  is the Cauchy stress tensor,  $\mathbf{b}$  is the body force,  $\rho$  is the density of the object, and  $d\mathbf{v}/dt$  is the rate of change of velocity. This leads to the stress equilibrium equation in terms of 2<sup>nd</sup> Piola-Kirchhoff stress in the reference coordinate system:

$$\frac{\partial}{\partial \mathbf{X}_k} (\mathbf{S}_{ki} \mathbf{F}_{ji}) = 0 \quad (6)$$

assuming there is no body force acting on the object and the gravity is neglected.

Furthermore, one can generate the virtual work by considering the traction force  $\mathbf{t}$  acting on the surface  $s$  and the body force  $\mathbf{b}$  acting on the volume  $v$ , and equating to the virtual work done by moving the object by an imaginary displacement  $\delta \mathbf{u}$  [4].

$$\int_s \mathbf{t} \cdot \delta \mathbf{u} ds + \int_v \mathbf{b} \cdot \delta \mathbf{u} dv = \int_v \boldsymbol{\sigma} : \delta \boldsymbol{\epsilon} dv + \int_v \rho \frac{d\mathbf{v}}{dt} \cdot \delta \mathbf{u} dv \quad (7)$$

From the principle of virtual work (in weak form), together with the stress equilibrium equation, the finite element model of soft tissue mechanics was constructed.

### 2.3 Contact Mechanics

To model the contact mechanics, introduced during compression, a penalty method was incorporated to the finite element model. In this method, a penalty term  $\Pi^p$ , defined by:

$$\Pi^p = \int_{s^c} \varepsilon_N \mathbf{g}_N \delta \mathbf{g}_N ds^c \quad (8)$$

due to the constraint condition was added to equation (7) [5].  $\varepsilon_N$  is the penalty parameter,  $\mathbf{g}_N$  is the penetration function and  $s^c$  is the active or contact surfaces. The penalty term is only added for the active constraints. The larger the penalty parameter, the more accuracy can be achieved, and as  $\varepsilon_N \rightarrow \infty$ , the

penalty method becomes a Lagrange multiplier method, although the system may be ill-conditioned at the same time. Note that this penalty method formulation does not include frictional effects.

## III. EXPERIMENTAL VALIDATION

### 3.1 Experimental Methodology

A phantom silicon gel cylinder was created with dimensions of 29 mm in diameter and 40 mm in length. The material response of this silicon gel was known to be isotropic, homogeneous and incompressible [6]. The cylinder gel was placed between two perspex plates and compressed to 17 mm thick, as shown in Figure i. The digital camera was used to quantify the deformed geometry of the gel to compare with the finite element model prediction of phantom deformation.

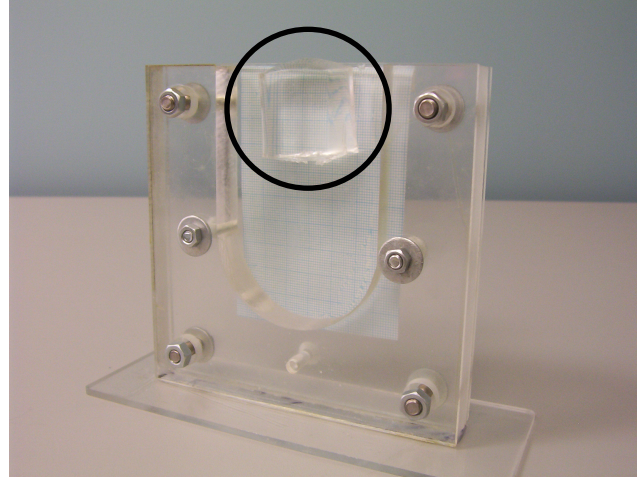


Figure i: The perspex plates used to apply compression to the phantom gel cylinder (circled).

### 3.2 Finite Element Model of Phantom Silicon Gel

Considering the deformation to be symmetric about the horizontal, only a half cylinder subject to compression by one plate was used to simulate the deformation of the phantom. The geometry of the phantom gel cylinder was interpolated using tri-cubic Hermite basis functions to generate a  $G_1$  continuous displacement field. This provided piecewise continuous strain fields across element boundaries, resulting in more accurate geometric solutions in comparison to lower order interpolation schemes [7].

The finite element model was constructed with the same dimensions as the phantom gel cylinder used in the experiment. It has previously been shown that the silicon phantom gel used to model the breast

can be described by a Neo-Hookean material law, in which the strain energy function is defined by

$$W = c_1(I_1 - 3) \quad (9)$$

where  $I_1$  is the first invariant of the right Cauchy-strain tensor and  $c_1$  was found to be 3 kPa for the phantom gel [6]. The plate was modelled as a rigid body.

### 3.3 Results

As can be seen in the Figure ii, the finite element model prediction of the phantom gel cylinder subject to compression by rigid plates matched the experimental data, with an error of less than 2 % in radial strain.

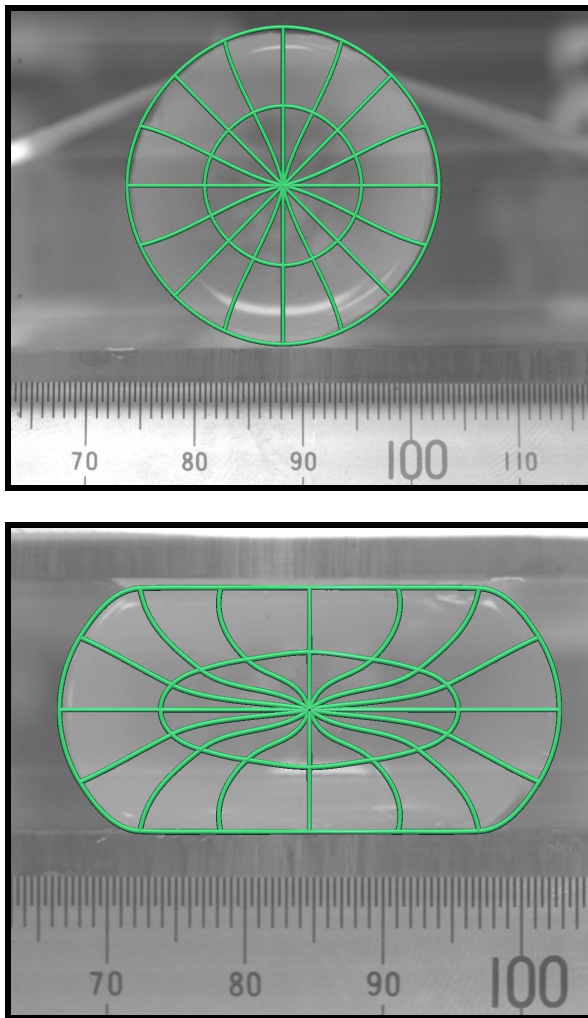


Figure ii: Phantom gel cylinder under compression by two rigid plates (top: undeformed, bottom: deformed). Thick lines illustrate the finite element model.

## IV. BREAST COMPRESSION DURING MAMMOGRAPHY

### 4.1 Model Generation

A semi-automatic procedure has been developed to fit customized finite element models of breast geometry to patient data segmented from magnetic resonance images (see Figure iii). This procedure accurately captures the geometry of the breast and also copes with the requirement to rapidly create models specific to the individual patients, which is important in clinical setting.

Magnetic resonance images of the breasts of individual patients are segmented into the various tissue components (e.g. skin, fibroglandular tissue, fatty tissue and any cancerous lesions). The geometry is approximated by using tri-cubic Hermite interpolation and fitted using a non-linear least squares method.

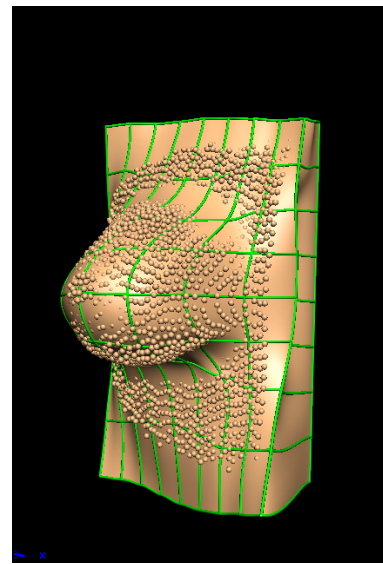
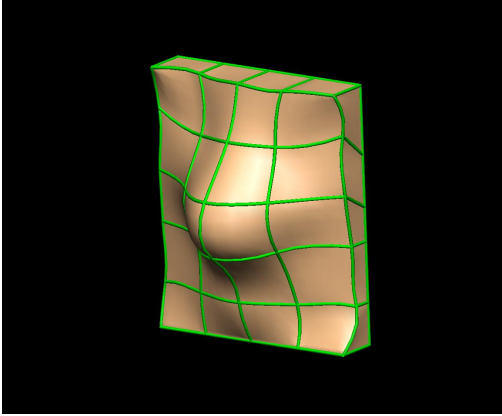


Figure iii: A patient specific finite element model created from a set of magnetic resonance images.

### 4.2 Modelling Breast Compression

We constructed a geometrically realistic phantom model of the breast from silicon gel (with known material properties) using a mould from a mannequin. The breast phantom was subject to CC compression loading using a custom-built rig. The surface geometry of the breast mould was laser-scanned to produce a dense set of 3D geometric data, to which an anatomical breast model was fitted using the above procedure (see Figure iv).



**Figure iv: A finite element mesh generated with laser-scanned data points.**

A contact mechanic framework was integrated to finite model to simulate mammographic compression of the breast phantom. The experimental deformations were used to assess the quality of the model predictions. These validation results justify the use of our finite element modelling framework to investigate clinical compression data from mammographic imaging studies in patients. The next step is to investigate the use of more accurate material laws of the various tissue types on the ability of the modelling framework to reliably track breast tumours.

## V. CONCLUSIONS

A finite element modelling framework has been developed to simulate compression of the breast using large deformation non-linear elasticity subject to contact mechanics loading conditions. Model prediction matched the experimental results for a cylinder silicon gel under compression. Anatomically accurate geometric models of the breasts were constructed and subject to contact compression to mimic the CC mammographic procedure. The comparison of model predictions with experimental data from phantoms validated this technique for an analysis of breast tissue deformation during mammography. The longer-term objective of this research is to develop a diagnostic tool to aid radiologists with the interpretation of mammograms and detection of tumours. The three-dimensional computational framework has potential to guide surgical procedures (such as biopsy), and to help patients to better understand their condition

## ACKNOWLEDGEMENT

J.H.Chung would like to thank the Bioengineering Institute for providing the opportunity to work on this project. The authors also thank Dr Ruth Warren MD, Consultant Radiologist University of Cambridge, and the staff of the breast and MRI department of Addenbrooke's Hospital, Cambridge UK for providing the breast MR data used in Figure iii.

## REFERENCES

1. D.Rueckert, L.Sonoda, C.Hayes, D.Hill, M.Leach, D.Hawkes, Nonrigid registration using free-form deformations: application to breast MR images, *IEEE Trans. Med. Imag.*, **18**, no. 8: 712-721, Aug 1999.
2. C.Tanner, J.Schnabel, A.Degenhard, A.Castellano-Smith, C.Hayes, M.Leach, D.Hose, D.Hill, D.J.Hawkes, Validation of volume-preserving non-rigid registration: Application to contrast-enhanced MR-mammography, In Medical Image Computing and Computer-Assisted Intervention (MICCAI 2002), Lecture notes in Computer science, 2489-I:307-314, Sep 2002.
3. R.J.Atkin, N.Fox, An introduction to the Theory of Elasticity, Longman Group Limited, 1980.
4. L.E.Malvern, Introduction to the Mechanics of a Continuous Medium, Prentice-Hall Inc, 1969.
5. P.Wriggers, Computational Contact Mechanics, Wiley, 2002.
6. V.Rajagopal, P.M.F.Nielsen, M.P.Nash, A 3D Finite Element Model of the Breast to Study Breast Cancer, WC2003 World Congress on Medical Physics and Biomedical Engineering, 2003.
7. M.P.Nash, P.J.Hunter, Computational mechanics of the heart, *J. Elasticity*, **61**:113-141,200